Research Article

Pharmacological Assessment Of Abrus Precatorius L. For Antidiabetic Activity With Molecular Docking Insights

Dinesh Shivram Padavi1, Dr. Vikas V. Patil2*

[1] Research Scholar, Department Pharmacognocy, KVPS's Institute of Pharmaceutical Education Boradi (Shirpur), Dhule – 425428, Affiliated with Kavayitri Bahinabai Chaudhari North Maharashtra University, Jalgaon (MH, India)
[2] Research Guide and Principal, Department Pharmacognocy, KVPS's Institute of Pharmaceutical Education Boradi (Shirpur), Dhule – 425428, Affiliated with Kavayitri Bahinabai Chaudhari North Maharashtra University, Jalgaon (MH, India), vikas312@rediffmail.com

Abstract

Diabetes mellitus is a major metabolic disorder characterized by impaired glucose regulation and alterations in insulin-related signalling pathways. Several molecular targets, including α-amylase, α-glucosidase, dipeptidyl peptidase-4 (DPP-4), protein tyrosine phosphatase 1B (PTP1B) and peroxisome proliferator-activated receptor gamma (PPAR-γ), are associated with glucose homeostasis and represent important targets for antidiabetic drug discovery. Phytoconstituents such as Abrine and Quercetin have attracted interest for their potential pharmacological relevance. The present study aimed to investigate the predicted binding interactions of Abrine and Quercetin with selected molecular targets associated with diabetes mellitus using molecular docking analysis. The molecular structures of Abrine and Quercetin were evaluated against selected protein targets, including α-glucosidase, α-amylase, DPP-4, PTP1B and PPAR-γ. Protein binding cavities were identified using CurPocket and molecular docking was performed to assess the predicted binding affinity of the selected phytoconstituents. The docking poses and binding interactions were further examined using Discovery Studio Visualizer. Abrine exhibited its most favourable predicted binding score against α-glucosidase (PDB ID: 3TOP), with a score of −7.4 kcal/mol, followed by DPP-4 (5J3J; −6.9 kcal/mol), α-amylase (4W93; −6.6 kcal/mol), PPAR-γ (2PRG; −6.6 kcal/mol) and PTP1B (2HNP; −6.0 kcal/mol). Quercetin demonstrated favourable predicted binding against α-glucosidase (3A4A), with a score of −8.5 kcal/mol, and α-amylase (5E0F), with a score of −7.5 kcal/mol. The results indicated that both compounds could be accommodated within selected binding cavities of the investigated proteins, although the predicted binding scores varied according to the target and binding-pocket characteristics. The molecular docking findings provide preliminary computational evidence supporting further investigation of Abrine and Quercetin against selected molecular targets associated with diabetes mellitus. Their predicted interactions with carbohydrate-digesting enzymes and other glucose-regulatory targets indicate potential relevance for antidiabetic drug discovery. Nevertheless, docking predictions alone cannot establish biological activity or therapeutic efficacy. Further validation through in vitro enzyme inhibition assays, molecular dynamics simulations and in vivo pharmacological studies is necessary to establish their antidiabetic potential.

Keywords: Abrus precatorius; Abrine; Quercetin; Diabetes mellitus; Molecular docking; α-Amylase; α-Glucosidase.

1. Introduction

Diabetes mellitus is a chronic metabolic disorder characterized by persistent hyperglycaemia resulting from impaired insulin secretion, defective insulin action or a combination of both mechanisms [1]. It represents a major global public health concern because of its increasing prevalence and association with several long-term complications, including cardiovascular disorders, diabetic nephropathy, retinopathy, neuropathy and impaired wound healing. The development of insulin resistance and progressive pancreatic β-cell dysfunction contributes significantly to the progression of the disease [2,3]. In addition to abnormalities in insulin-mediated glucose metabolism, disturbances in carbohydrate digestion, glucose absorption, lipid metabolism and intracellular signalling pathways further contribute to metabolic imbalance [4]. Although several pharmacological agents are currently available for diabetes management, their therapeutic limitations, adverse effects and the need for long-term treatment have encouraged continued research into alternative therapeutic resources, particularly plant-derived bioactive compounds [5-7].

The regulation of postprandial blood glucose is an important therapeutic approach in the management of type 2 diabetes mellitus. Enzymes such as α-amylase and α-glucosidase play essential roles in carbohydrate digestion by facilitating the breakdown of complex carbohydrates into absorbable monosaccharides [8]. Inhibition of these enzymes

can delay carbohydrate digestion and glucose absorption, thereby reducing postprandial hyperglycaemia. Similarly, dipeptidyl peptidase-4 (DPP-4) is an important therapeutic target because it promotes the degradation of incretin hormones, including glucagon-like peptide-1 (GLP-1), which regulate glucose-dependent insulin secretion [9]. Peroxisome proliferator-activated receptor gamma (PPAR-γ), a nuclear receptor involved in glucose and lipid homeostasis, represents another important target because of its regulatory role in insulin sensitivity and adipocyte metabolism [10-13]. Furthermore, protein tyrosine phosphatase 1B (PTP1B) negatively regulates insulin receptor signalling and has been investigated as a potential target for improving insulin sensitivity. Therefore, exploring bioactive compounds capable of interacting with these molecular targets may provide useful insights into their possible antidiabetic mechanisms [14]. Medicinal plants represent an important source of structurally diverse secondary metabolites with potential therapeutic applications in metabolic disorders. Their pharmacological properties are commonly associated with different classes of phytochemicals, including alkaloids, flavonoids, phenolic compounds, terpenoids, tannins and saponins [15,16].

Abrus precatorius L., belonging to the family Fabaceae, is a medicinal plant widely distributed across tropical and subtropical regions. Commonly known as rosary pea or Gunja, the plant has a long history of traditional medicinal applications in different systems of healthcare [17,18]. Various plant parts, including leaves, roots, and seeds, have been investigated for their phytochemical composition and pharmacological properties [19]. Previous investigations have reported the presence of several chemical constituents, including alkaloids, flavonoids, phenolic compounds, triterpenoids, steroids, saponins and other secondary metabolites [20,21]. Reported pharmacological activities of A. precatorius include antioxidant, anti-inflammatory, antimicrobial, antitumour, immunomodulatory and antidiabetic effects [22-25]. The diversity of its chemical constituents and reported biological activities indicates that this plant may serve as a valuable source of compounds for further pharmacological investigation [26,27].

Among the phytochemical constituents associated with A. precatorius, abrine and quercetin are of particular interest in the present investigation. Abrine, chemically identified as N-methyltryptophan, is an indole-derived alkaloid reported from different parts of the plant, including its leaves and seeds [28]. Its occurrence has been documented in phytochemical investigations of A. precatorius, supporting its consideration as a plant-associated constituent for further biological evaluation. Quercetin, a naturally occurring flavonol belonging to the flavonoid class, has also been reported in phytochemical records associated with A. precatorius [29]. Quercetin is widely investigated for its antioxidant and metabolic regulatory properties, particularly its potential influence on glucose metabolism, carbohydrate-digesting enzymes and insulin-associated signalling pathways [30]. The different chemical structures of abrine and quercetin provide an interesting basis for examining their possible interactions with selected proteins involved in glucose regulation and insulin sensitivity [31,32].

Molecular docking is a computational approach widely employed in drug discovery to investigate the possible binding orientation and interaction patterns of small molecules within the active or binding sites of target proteins. In antidiabetic research, molecular docking can be particularly useful for exploring the potential interactions of phytochemicals with enzymes and proteins involved in carbohydrate digestion, incretin regulation, insulin signalling and metabolic homeostasis [33,34]. Abrine was evaluated against α-glucosidase (PDB ID: 3TOP), α-amylase (PDB ID: 4W93), DPP-4 (PDB ID: 5J3J), PPAR-γ (PDB ID: 2PRG) and PTP1B (PDB ID: 2HNP). Quercetin was investigated against α-amylase (PDB ID: 5E0F) and α-glucosidase (PDB ID: 3A4A). This target-based computational assessment was intended to provide additional insights into the possible molecular interactions of the selected phytochemicals with proteins associated with carbohydrate metabolism and insulin-related pathways [35].

Considering the reported phytochemical diversity and pharmacological relevance of A. precatorius, the present study was designed to assess its antidiabetic potential through phytochemical investigation and pharmacological screening, complemented by molecular docking analysis of selected plant-associated compounds. The computational investigation focused on abrine and quercetin to explore their predicted interactions with relevant antidiabetic molecular targets.

2. Materials And Methods

2.1 Collection and Authentication of Plant Material

The seeds of Abrus precatorius L. were selected for the present pharmacological investigation was obtained in dried

form and subsequently processed for extraction. Botanical authentication of the plant was carried out by the Department of Botany, S.N.J.B.'s K.K.H.A. Arts, S.M.G.L. Commerce and S.P.H.J. Science College, Chandwad, District Nashik, Maharashtra, India. Based on the morphological and microscopic examination of the fresh, dried and market-sourced plant material, the specimen was identified as Abrus precatorius L., belonging to the family Fabaceae. The regional name of the plant was recorded as Gunja.

2.2 Preparation of Petroleum Ether Extract

The dried seeds of Abrus precatorius were processed into powder and approximately 50 g of the powdered material was accurately weighed. The powdered material was placed in a suitable cellulose extraction thimble and positioned inside the Soxhlet extraction chamber [36]. The Soxhlet apparatus was assembled with a round-bottom flask and water-cooled condenser, ensuring appropriate connections throughout the system. Petroleum ether (40–50°C) was used as the extraction solvent. The solvent was placed in the round-bottom flask and extraction was performed. During extraction, the solvent underwent repeated cycles of vaporization, condensation and siphoning, allowing the solvent to come into contact with the powdered plant material. The extraction process was continued for approximately 6–8 hours. Following completion of the extraction, the apparatus was allowed to cool before the extract-containing solvent was collected. The petroleum ether extract was separated from the extraction assembly and transferred into a suitable labelled container [37]. The solvent was subsequently removed using an appropriate solvent-recovery procedure and resulting extract (3.11% yield) was stored in a properly labelled, sealed container under suitable conditions.

3. Molecular Docking Studies

3.1 Selection and Preparation of Ligands (Abrine and Quercetin)

Abrine and quercetin were selected as the phytochemical compounds associated with Abrus precatorius L. for molecular docking investigation to explore their potential interactions with selected proteins involved in diabetes-related metabolic pathways. Abrine, an indole-derived alkaloid and quercetin, a naturally occurring flavonoid, possess distinct chemical structures that provide a basis for evaluating their possible interactions with different molecular targets associated with glucose metabolism and insulin regulation. The three-dimensional chemical structures of abrine and quercetin were obtained from PubChem database in PDB format [38]. The downloaded ligand structures were imported into AutoDock Vina for ligand preparation. was performed to Structural optimization obtain suitable three-dimensional conformations before molecular docking. Hydrogen atoms were added wherever required and appropriate protonation states and partial charges were assigned [39]. The prepared ligand structures were subsequently converted into the required docking-compatible format for further computational analysis.

3.2 Selection and Preparation of Target Proteins

Five proteins associated with glucose metabolism and insulin-related signalling pathways were selected as molecular docking targets for abrine, while two carbohydrate-digesting enzymes were selected for quercetin. The three-dimensional crystal structures of the selected proteins were retrieved from the Research Collaboratory for Structural Bioinformatics Protein Data Bank (RCSB PDB) using their respective Protein Data Bank identification codes [40,41]. The selected protein structures were prepared before docking to obtain suitable receptor conformations. Protein preparation involved examination of the downloaded structures, selection of the appropriate protein chain, removal of non-essential water molecules where appropriate and removal of co-crystallized ligands when required for the docking procedure. Polar hydrogen atoms and appropriate atomic charges were subsequently assigned [42]. The prepared receptor structures were converted into the required docking-compatible format for subsequent ligand–protein interaction studies. The selected molecular targets and their corresponding PDB identification codes are presented in Table 1.

Table 1. Selected Molecular Targets for Molecular Docking Investigation

No.	Ligand	Molecular target	PDB ID
1	Abrine	α-Glucosidase	3TOP
2	Abrine	α-Amylase	4W93
3	Abrine	DPP-4	5J3J
4	Abrine	PPAR-γ	2PRG

5	Abrine	PTP1B	2HNP
6	Quercetin	α-Amylase	5E0F
7	Quercetin	α-Glucosidase	3A4A

3.2 Molecular Docking of Abrine

Molecular docking of abrine was performed against five selected molecular targets, namely α-glucosidase (PDB ID: 3TOP), α-amylase (PDB ID: 4W93), dipeptidyl peptidase-4 (DPP-4; PDB ID: 5J3J), peroxisome proliferator-activated receptor gamma (PPAR-γ; PDB ID: 2PRG) and protein tyrosine phosphatase 1B (PTP1B; PDB ID: 2HNP). The prepared three-dimensional structure of abrine was docked individually into the selected protein binding sites to investigate its potential binding orientation and molecular interactions. The docking procedure was performed using CurPocket. The binding site for each receptor was defined based on specified grid coordinates. Docking calculations were conducted using the selected search parameters to identify favourable ligand-binding conformations. The generated docking poses were evaluated based on their predicted binding affinity scores and interaction patterns within the respective protein binding sites. The best-ranked docking conformations were selected for subsequent analysis of ligand–protein interactions. This approach was used to explore the possible involvement of abrine in carbohydrate digestion, incretin regulation, and insulin-associated signalling pathways.

3.3 Molecular Docking of Quercetin

Quercetin was subjected to molecular docking against two carbohydrate-metabolizing enzymes, namely α-amylase (PDB ID: 5E0F) and α-glucosidase (PDB ID: 3A4A). These enzymes were selected because of their important roles in the enzymatic breakdown of dietary carbohydrates and regulation of postprandial blood glucose levels. The prepared three-dimensional structure of quercetin was docked individually against the selected protein targets using CurPocket. The respective binding sites were defined according to the selected receptor structures and their reference binding-site information. Docking calculations were performed to identify favourable binding orientations and estimate the binding affinity of quercetin towards each selected enzyme. The generated docking conformations were assessed according to their predicted binding scores and molecular interaction profiles. The best-ranked poses were selected to investigate the possible interactions of quercetin with amino acid residues located within the binding pockets of α-amylase and α-glucosidase. The resulting computational findings were considered complementary evidence for evaluating the potential antidiabetic relevance of quercetin [43].

3.4 Analysis of Ligand–Protein Interactions

The ligand–protein interaction profiles of abrine and quercetin were analysed to identify the amino acid residues involved in molecular recognition and binding within the selected protein structures. The best-ranked docking conformations were visualized using CurPocket to examine the orientation of each ligand within its corresponding protein-binding pocket. Different types of non-covalent interactions, including hydrogen bonding, hydrophobic interactions, van der Waals interactions and other relevant intermolecular contacts, were examined [44]. The interacting amino acid residues and their corresponding interaction distances were recorded wherever available. Two-dimensional and three-dimensional interaction diagrams were generated to illustrate the binding orientations and molecular interaction patterns of the selected phytochemicals with their respective targets. The docking scores and observed interaction profiles were compared across the selected protein targets to obtain preliminary insights into the molecular recognition behaviour of abrine and quercetin [40,44]. These findings were interpreted in relation to the biological functions of the selected proteins and their relevance to glucose metabolism and insulin signalling.

4. Result And Discussion

4.1 Molecular Docking Analysis of Abrine against α-Glucosidase (PDB ID: 3TOP)

The protein structure was selected as a molecular target owing to the physiological importance of α-glucosidase in the terminal digestion of carbohydrates and its relevance to the regulation of postprandial blood glucose levels. The identification of suitable ligand-binding cavities was performed using CurPocket, which enabled the evaluation of multiple predicted binding regions within the protein structure. Five binding pockets (C1–C5) were identified and evaluated for Abrine binding using AutoDock Vina. The docking grid was defined for each pocket using the

corresponding centre coordinates and spatial dimensions expressed in angstroms (Å). The predicted docking energies and pocket characteristics are summarized in Table 2.

Table 2. Molecular docking analysis of Abrine against α-glucosidase (PDB ID: 3TOP)

Pocket ID	Docking energy (kcal/mol)	Pocket volume (Å³)	Pocket centre (x, y, z) (Å)	Grid dimensions (Å)
C4	−7.4	727	(−55, 7, −72)	19 × 19 × 19
C3	−6.5	783	(−41, 0, −13)	19 × 19 × 19
C1	−5.6	1686	(−1, 0, −49)	19 × 26 × 19
C2	−5.6	1348	(−81, 13, 19)	19 × 19 × 25
C5	−5.2	605	(−33, 22, −55)	19 × 19 × 19

Among the five predicted binding pockets, C4 demonstrated the most favourable docking energy of −7.4 kcal/mol, followed by C3 with a docking energy of −6.5 kcal/mol. Pockets C1 and C2 exhibited identical docking energies of −5.6 kcal/mol, whereas C5 showed the least favourable docking energy of −5.2 kcal/mol. The comparatively lower docking energy obtained for C4 suggests a more favourable predicted interaction of Abrine with this binding cavity than with the other identified pockets.

Pocket C4 exhibited a cavity volume of 727 Å³, whereas C3 possessed a slightly larger volume of 783 Å³. Despite the difference in pocket volume, C4 demonstrated a more favourable docking energy, suggesting that the spatial arrangement and physicochemical characteristics of the binding cavity may influence ligand accommodation and predicted binding stability. In contrast, C1 and C2 possessed substantially larger cavity volumes of 1686 and 1348 Å³, respectively, but showed comparatively less favourable docking energies. These observations indicate that cavity size alone may not determine ligand-binding behaviour, as the interaction is also influenced by the structural and chemical environment of the binding region. The docking results further demonstrated that Abrine could be accommodated within different predicted cavities of α-glucosidase, although the calculated docking energies varied between the pockets. The comparatively favourable result obtained for C4 suggests that this pocket may provide a suitable environment for Abrine binding.

The favourable predicted interaction of Abrine with α-glucosidase may be pharmacologically relevant because inhibition of this enzyme can delay the hydrolysis of dietary carbohydrates into absorbable glucose. Such inhibition may contribute to the attenuation of postprandial glucose elevation. Nevertheless, the docking energy obtained in the present study represents a computational prediction and cannot independently establish enzyme inhibition, competitive binding, or antidiabetic efficacy. Overall, the molecular docking analysis identified Pocket C4 as the most favourable predicted binding cavity for Abrine against α-glucosidase (PDB ID: 3TOP), with a docking energy of −7.4 kcal/mol.

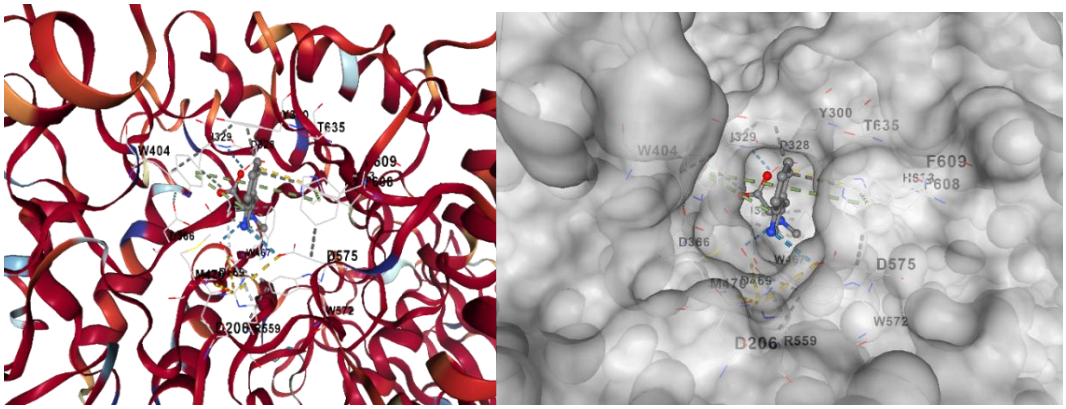

Figure 1. Representation Showing the Binding Orientation and Accommodation of Abrine with α-Glucosidase (PDB ID: 3TOP)

4.2 Molecular Docking Analysis of Abrine against α-Amylase (PDB ID: 4W93)

α-amylase can delay carbohydrate digestion and may reduce the rate of postprandial glucose elevation, making it an important target in the management of type 2 diabetes mellitus. The human pancreatic α-amylase structure (PDB ID: 4W93) was selected for the molecular docking investigation of Abrine. The selected structure is an X-ray crystallographic structure of human pancreatic α-amylase complexed with montbretin A, resolved at 1.35 Å, providing Amylase is an important digestive enzyme responsible for the hydrolysis of starch into smaller carbohydrate molecules. Inhibition of a structurally well-defined model for docking analysis. Five potential binding pockets (C1–C5) identified using CurPocket were evaluated for the interaction of Abrine with α-amylase using AutoDock Vina. The corresponding grid dimensions were maintained at 19 × 19 × 19 Å for all five pockets. The predicted docking energies, pocket volumes, pocket-centre coordinates and grid dimensions are presented in Table 3.

Table 3. Molecular docking analysis of Abrine against α-amylase (PDB ID: 4W93)

Pocket ID	Docking energy (kcal/mol)	Pocket volume (Å³)	Pocket centre (x, y, z) (Å)	Grid dimensions (Å)
C1	−6.6	365	(−12, 1, −24)	19 × 19 × 19
C3	−6.3	229	(−15, 32, −9)	19 × 19 × 19
C5	−6.1	106	(−11, 13, −35)	19 × 19 × 19
C2	−5.8	349	(−2, 38, −29)	19 × 19 × 19
C4	−5.7	148	(−7, 5, −30)	19 × 19 × 19

Among the evaluated binding cavities, Pocket C1 demonstrated the most favorable docking energy of −6.6 kcal/mol, followed by C3 (−6.3 kcal/mol) and C5 (−6.1 kcal/mol). Pockets C2 and C4 exhibited docking energies of −5.8 and −5.7 kcal/mol, respectively. These findings indicate that Abrine demonstrated variation in predicted binding behavior across the five cavities, with C1 representing the most favorable docking site among those evaluated. Pocket C1 exhibited a volume of 365 Å³, which was the largest among the five predicted cavities, followed closely by C2 with a volume of 349 Å³. Despite the similar cavity volumes, C1 demonstrated a more favorable docking energy than C2. This difference may be associated with the structural arrangement and physicochemical properties of the respective binding environments. The comparatively favorable score obtained for C1 suggests that this pocket may provide a suitable environment for Abrine accommodation and ligand–protein interaction.

Pocket C3, with a cavity volume of 229 Å³, exhibited the second-most favorable docking energy of −6.3 kcal/mol. Interestingly, Pocket C5 showed a docking energy of −6.1 kcal/mol despite possessing the smallest cavity volume (106 Å³). This observation suggests that a smaller cavity may still support a favorable predicted ligand interaction depending on its shape, amino acid composition and ligand orientation. In comparison, Pocket C4 demonstrated the least favorable docking energy (−5.7 kcal/mol) among the evaluated pockets. The docking results indicate that cavity size alone does not determine the predicted interaction strength. Rather, the relative arrangement of residues within the binding region and the physicochemical compatibility between the ligand and the pocket may influence the docking score. Although C1 was the largest cavity and demonstrated the most favorable docking energy in the present analysis, confirmation of the specific molecular interactions requires detailed examination of the docked ligand orientation and interacting residues.

Overall, Abrine exhibited the most favorable predicted interaction with α-amylase at Pocket C1, with a docking energy of −6.6 kcal/mol and a cavity volume of 365 Å³. The results provide preliminary computational evidence for a possible interaction between Abrine and human pancreatic α-amylase. Further investigation through ligand–protein interaction mapping and in vitro α-amylase inhibition assays is required to establish the functional significance of this interaction and its potential contribution to antidiabetic activity.

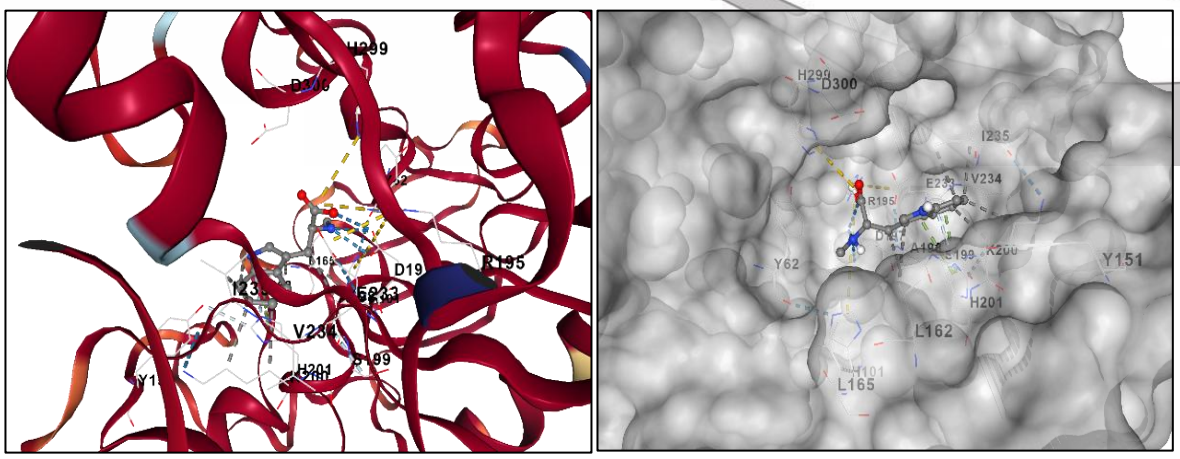

Figure 2. Representation Showing the Binding Orientation and Accommodation of Abrine with α-Amylase (PDB ID: 4W93)

4.3 Molecular Docking Analysis of Abrine against Dipeptidyl Peptidase-4 (DPP-4; PDB ID: 5J3J)

Dipeptidyl peptidase-4 (DPP-4) is an important enzyme involved in the regulation of glucose homeostasis through the degradation of incretin hormones, particularly glucagon-like peptide-1 (GLP-1) and glucose-dependent insulinotropic polypeptide (GIP). Inhibition of DPP-4 prevents the rapid degradation of incretins, thereby prolonging their biological activity and supporting improved glycaemic regulation. Consequently, DPP-4 represents an established therapeutic target for the management of type 2 diabetes mellitus.

The crystal structure with PDB ID 5J3J was selected to investigate the potential interaction of Abrine with human DPP-4. According to the RCSB Protein Data Bank, this structure represents human DPP-IV in complex with the small-molecule inhibitor HL1 and was determined by X-ray diffraction at a resolution of 2.75 Å. The availability of a crystallographically characterized protein structure provides a suitable structural reference for investigating ligand–protein interactions. Five potential binding cavities (C1–C5) were identified using CurPocket and evaluated for Abrine binding through molecular docking using AutoDock Vina. The corresponding docking energies, pocket volumes, pocket-centre coordinates and grid dimensions are presented in Table 4.

Table 4. Molecular docking analysis of Abrine against DPP-4 (PDB ID: 5J3J)

Pocket ID	Docking energy (kcal/mol)	Pocket volume (Å³)	Pocket centre (x, y, z) (Å)	Grid dimensions (Å)
C3	−6.9	1136	(21, −16, 102)	25 × 19 × 27
C1	−6.4	2316	(2, 9, 48)	26 × 25 × 32
C4	−6.4	630	(8, −14, 49)	19 × 19 × 19
C2	−5.9	1216	(25, 6, 39)	29 × 19 × 19
C5	−5.9	602	(45, −5, 105)	19 × 19 × 19

The molecular docking results demonstrated variation in the predicted interaction of Abrine across the five identified binding cavities of DPP-4. Among these, Pocket C3 exhibited the most favourable docking energy of −6.9 kcal/mol, indicating the strongest predicted interaction among the evaluated pockets. Pocket C1 and Pocket C4 showed identical docking energies of −6.4 kcal/mol, whereas Pockets C2 and C5 demonstrated docking energies of −5.9 kcal/mol. Pocket C3 possessed a cavity volume of 1136 Å³, providing a relatively spacious binding environment for ligand accommodation. Its comparatively favourable docking energy suggests that the structural and physicochemical characteristics of this cavity may support a favourable interaction with Abrine. However, the docking score alone cannot establish whether C3 represents the catalytic region of DPP-4 or whether the ligand interacts directly with the catalytic residues.

Pocket C1 exhibited the largest cavity volume of 2316 Å³ among the evaluated binding regions, with a docking energy of −6.4 kcal/mol. Although the larger cavity may provide greater spatial accommodation, its predicted interaction was less favourable than that observed in C3. Similarly, Pocket C2 possessed a volume of 1216 Å³ but demonstrated a

docking energy of −5.9 kcal/mol. These findings indicate that cavity volume alone does not determine the predicted ligand-binding strength, as the arrangement of amino acid residues and the physicochemical environment of the binding region may also influence ligand accommodation. Interestingly, Pocket C4 demonstrated a docking energy of −6.4 kcal/mol despite having a relatively compact cavity volume of 630 Å³. This observation suggests that a smaller binding cavity may also provide a suitable environment for ligand interaction. Pocket C5, with a volume of 602 Å³, exhibited a docking energy of −5.9 kcal/mol, indicating a comparatively less favourable predicted interaction. Overall, molecular docking analysis identified Pocket C3 as the most favourable predicted binding cavity for Abrine against DPP-4 (PDB ID: 5J3J), with a docking energy of −6.9 kcal/mol and a pocket volume of 1136 Å³. The results provide preliminary computational support for investigating Abrine as a potential DPP-4-interacting phytochemical.

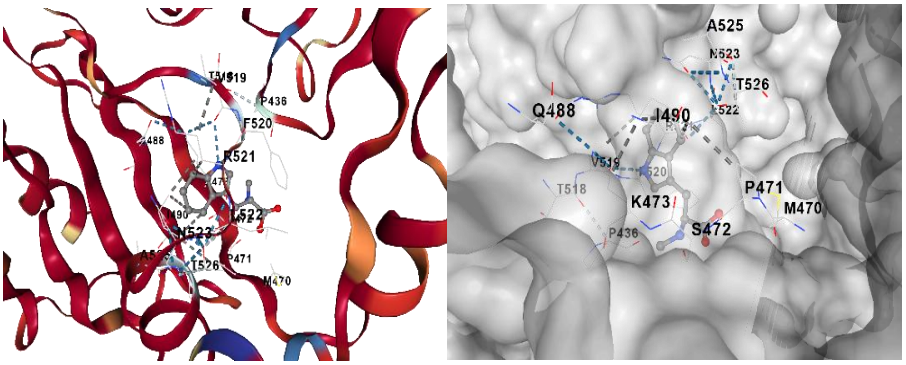

Figure 3. Representation Showing the Binding Orientation and Accommodation of Abrine with DPP-4 (PDB ID: 5J3J)

4.4 Molecular Docking Analysis of Abrine against PPAR-γ (PDB ID: 2PRG)

Peroxisome proliferator-activated receptor gamma (PPAR-γ) is a ligand-dependent nuclear receptor involved in the regulation of glucose homeostasis, lipid metabolism, adipocyte differentiation and insulin sensitivity. Activation of PPAR-γ influences the expression of genes associated with glucose and lipid metabolism and contributes to improved insulin responsiveness. The crystal structure with PDB ID 2PRG was selected to investigate the potential interaction of Abrine with the ligand-binding domain (LBD) of human PPAR-γ. According to the RCSB Protein Data Bank, this structure represents the human PPAR-γ ligand-binding domain in complex with the antidiabetic ligand rosiglitazone and a coactivator peptide. The structure was determined using X-ray crystallography at a resolution of 2.30 Å, providing a structurally characterized model for ligand-binding investigations. Five potential binding cavities (C1–C5) were identified using CurPocket and evaluated for Abrine binding through molecular docking using AutoDock Vina. The predicted docking energies, pocket volumes, pocket-centre coordinates and grid dimensions are summarized in Table 5.

Table 5. Molecular docking analysis of Abrine against PPAR-γ (PDB ID: 2PRG)

Pocket ID	Docking energy (kcal/mol)	Pocket volume (Å³)	Pocket centre (x, y, z) (Å)	Grid dimensions (Å)
C4	−6.6	398	(66, −9, 22)	19 × 19 × 19
C1	−6.5	10,902	(51, −19, 32)	35 × 32 × 35
C2	−6.2	2,883	(51, −42, 11)	35 × 19 × 25
C3	−5.4	748	(61, 1, 15)	19 × 19 × 19
C5	−5.1	264	(34, −24, 6)	19 × 19 × 19

Among the evaluated pockets, C4 exhibited the most favourable docking energy of −6.6 kcal/mol, followed closely by C1 with a docking energy of −6.5 kcal/mol. Pocket C2 showed a docking energy of −6.2 kcal/mol, whereas C3 and C5 exhibited comparatively less favourable values of −5.4 and −5.1 kcal/mol, respectively. These findings indicate that Abrine demonstrated different predicted binding behaviour depending on the structural characteristics of the selected binding cavity. Pocket C4 exhibited a cavity volume of 398 Å³ and produced the most favorable docking energy (−6.6 kcal/mol). Although this cavity was relatively compact, its docking result suggests that the binding environment may provide suitable physicochemical complementarity for Abrine accommodation. The relatively favourable docking energy obtained in this pocket indicates a potentially favourable ligand–protein interaction, although the specific intermolecular interactions require confirmation through residue-level analysis.

Pocket C1 possessed the largest predicted cavity volume of 10,902 Å³ and demonstrated a docking energy of −6.5 kcal/mol. Despite its exceptionally large volume, the docking energy was slightly less favourable than that obtained in C4. Pocket C2 also exhibited a relatively large cavity volume of 2,883 Å³, with a docking energy of −6.2 kcal/mol. These findings indicate that the predicted docking energy is not determined solely by cavity volume. Pocket C3, with a cavity volume of 748 Å³, exhibited a docking energy of −5.4 kcal/mol, whereas Pocket C5 showed the least favourable docking energy of −5.1 kcal/mol with a volume of 264 Å³. The comparatively less favourable docking energies observed in these cavities suggest that their structural environments may provide less favourable interactions for Abrine under the applied docking conditions.The overall docking analysis identified Pocket C4 as the most favourable predicted binding cavity for Abrine among the five evaluated regions.

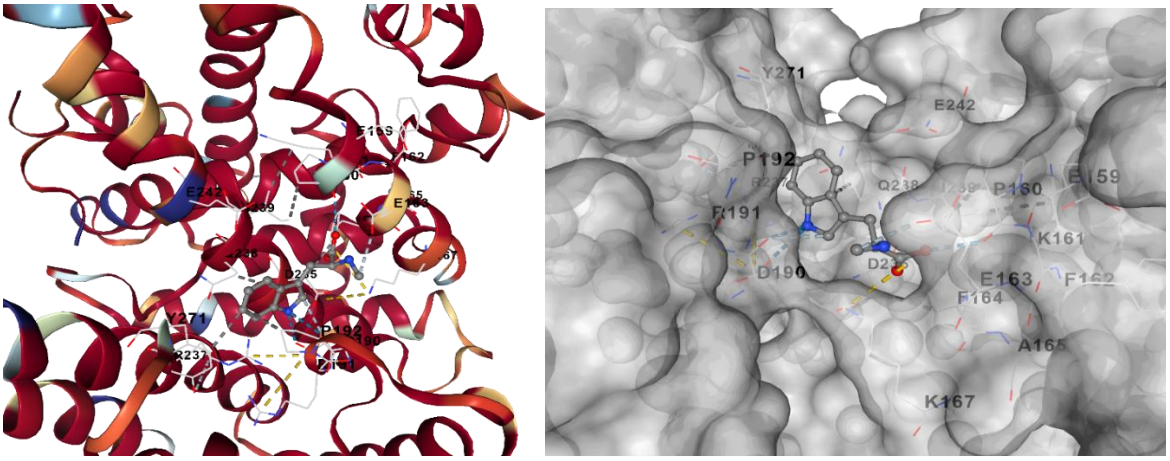

Figure 4. Representation Showing the Binding Orientation and Accommodation of Abrine with PPAR-γ (PDB ID: 2PRG)

4.5 Molecular Docking Analysis of Abrine against Protein Tyrosine Phosphatase 1B (PTP1B; PDB ID: 2HNP)

Protein Tyrosine Phosphatase 1B (PTP1B), encoded by the PTPN1 gene, is a cytosolic protein tyrosine phosphatase involved in the negative regulation of insulin signalling. Consequently, PTP1B has received considerable attention as a potential therapeutic target for improving insulin sensitivity and glucose homeostasis. The crystal structure of human PTP1B (PDB ID: 2HNP) was selected for the present molecular docking investigation. According to the RCSB Protein Data Bank, this structure was determined by X-ray diffraction at a resolution of 2.85 Å and represents the human PTP1B protein. Its catalytic site is located at the base of a shallow cleft, which provides a structural basis for investigating ligand interactions with the phosphatase.

Table 6. CurPocket analysis and molecular docking results of Abrine against PTP1B (PDB ID: 2HNP)

CurPocket ID	Docking energy (kcal/mol)	Pocket volume (Å³)	Pocket centre (x, y, z)	Grid dimensions (Å)
C1	−6.0	504	(49, 21, 3)	19 × 19 × 19
C2	−5.9	269	(45, 12, 28)	19 × 19 × 19
C3	−5.9	199	(65, 19, 21)	19 × 19 × 19
C5	−5.9	171	(54, 7, 24)	19 × 19 × 19
C4	−5.5	183	(39, 5, 22)	19 × 19 × 19

The docking analysis revealed predicted docking energies ranging from −5.5 to −6.0 kcal/mol across the five CurPocket-identified cavities. Among these, pocket C1 exhibited the most favourable docking energy (−6.0 kcal/mol), followed by C2, C3 and C5, which each showed an energy of −5.9 kcal/mol. Pocket C4 demonstrated the least favourable docking energy, at −5.5 kcal/mol. The comparatively favourable docking result for C1 suggests that Abrine may establish a more energetically favourable predicted interaction within this cavity under the applied docking conditions. C1 also exhibited the largest pocket volume (504 Å³), whereas C2, C3, C4 and C5 showed volumes of 269, 199, 183 and 171 Å³, respectively. These findings indicate that C1 provides the largest predicted cavity among the identified pockets. However, pocket volume alone cannot establish binding stability or identify the catalytic site; the ligand orientation and specific amino acid interactions must also be considered.

The similar docking energies obtained for C2, C3 and C5 indicate that Abrine produced comparable docking scores in these predicted cavities. In contrast, C4 exhibited a relatively less favourable score. Overall, C1 was the most favourable pocket among those evaluated, although confirmation that it corresponds to the PTP1B catalytic region requires examination of its position relative to the known catalytic residues. The CurPocket analysis identified differences in the spatial dimensions of the five predicted binding cavities. Pocket C1 showed the largest volume (504 Å³), followed by C2 (269 Å³), C3 (199 Å³), C4 (183 Å³) and C5 (171 Å³). These values describe the predicted spatial capacity of each cavity and provide information about the potential accommodation of Abrine. A grid dimension of 19 × 19 × 19 Å was applied to all five pockets. The corresponding grid centres were positioned according to the coordinates listed in Table 6.

PTP1B is an important negative regulator of insulin signalling. Its catalytic activity contributes to the dephosphorylation of the insulin receptor and attenuation of downstream signalling. Therefore, compounds capable of inhibiting PTP1B may potentially preserve insulin receptor phosphorylation and support insulin-mediated metabolic responses. In the present study, Abrine exhibited a most favourable predicted docking energy of −6.0 kcal/mol in pocket C1. This result provides preliminary computational evidence of a possible interaction between Abrine and PTP1B. If subsequent experiments establish that Abrine inhibits PTP1B catalytic activity, such inhibition could potentially contribute to enhanced insulin signalling and improved insulin sensitivity. However, the docking result alone does not demonstrate that Abrine inhibits PTP1B or that the predicted interaction occurs at its catalytic site. Further evaluation of the ligand-binding orientation, interacting amino acid residues and overlap with the established catalytic region is necessary to clarify the possible mechanism.

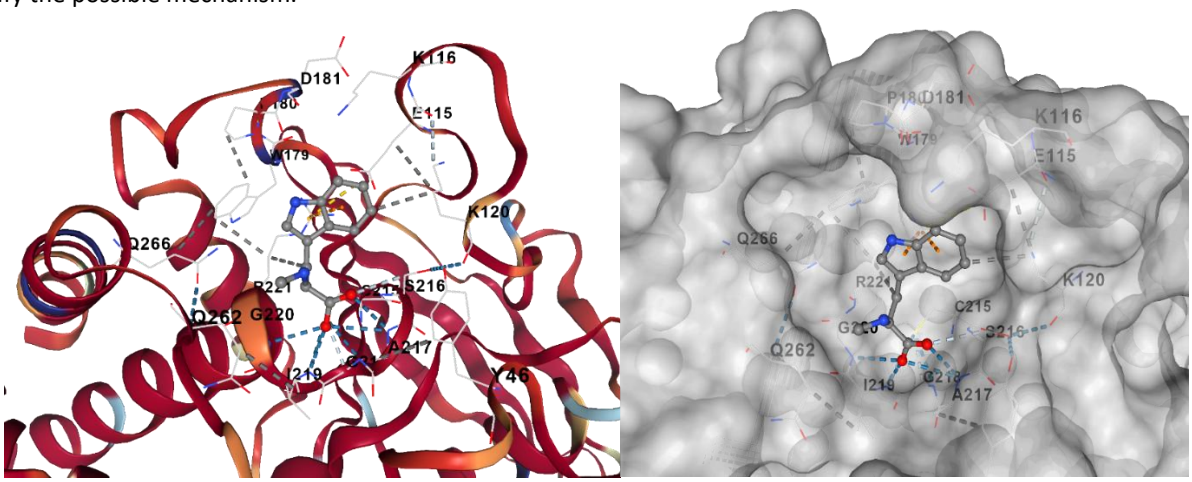

Figure 5. Representation Showing the Binding Orientation and Accommodation of Abrine with PTP1B (PDB ID: 2HNP)

4.6 Molecular Docking Analysis of Quercetin against α-Amylase (PDB ID: 5E0F)

α-Amylase is a major digestive enzyme responsible for the initial hydrolysis of dietary starch into maltose, maltotriose and smaller oligosaccharides. These products are subsequently processed by intestinal enzymes to produce absorbable monosaccharides. Inhibition of pancreatic α-amylase can delay carbohydrate digestion and may help reduce postprandial increases in blood glucose. Therefore, α-amylase is an important target in the investigation of potential antidiabetic compounds. The crystal structure PDB ID: 5E0F was selected for the present docking investigation. The RCSB Protein Data Bank identifies this structure as human pancreatic α-amylase in complex with mini-montbretin A, an established α-amylase inhibitor. The structure was determined by X-ray diffraction at a resolution of 1.40 Å and contains a 496-residue protein chain. Five predicted pockets (C1–C5) were evaluated. The docking energies, pocket volumes, pocket-centre coordinates and grid dimensions are summarized in Table 7.

Table 7. CurPocket analysis and molecular docking results of Quercetin against α-amylase (PDB ID: 5E0F)

CurPocket ID	Docking energy (kcal/mol)	Pocket volume (Å³)	Pocket centre (x, y, z)	Grid dimensions (Å)
C5	−7.5	142	(0, 38, −28)	21 × 21 × 21
C2	−7.2	307	(−9, 11, −33)	21 × 21 × 21
C3	−7.2	175	(−14, 31, −7)	21 × 21 × 21
C4	−7.2	175	(−6, 44, −21)	21 × 21 × 21

C1	−6.7	372	(−15, 3, −24)	21 × 21 × 21

The molecular docking analysis showed predicted docking energies ranging from −6.7 to −7.5 kcal/mol across the five CurPocket-identified cavities. Pocket C5 exhibited the most favourable docking energy (−7.5 kcal/mol), indicating the lowest predicted docking energy among the evaluated pockets. Pockets C2, C3 and C4 showed identical docking energies of −7.2 kcal/mol, while C1 exhibited a comparatively less favourable value of −6.7 kcal/mol. Interestingly, C5 had the smallest predicted pocket volume (142 Å³), whereas C1 had the largest volume (372 Å³). Despite its smaller volume, C5 produced the most favourable docking score. This observation suggests that cavity volume alone does not determine the predicted docking energy; ligand orientation, chemical complementarity and interactions with the surrounding residues may also influence the docking result. The comparable docking scores obtained for C2, C3 and C4 indicate that these cavities may also accommodate Quercetin in energetically similar predicted poses. However, the most favourable score in C5 identifies it as the leading candidate among the five evaluated pockets. Confirmation of its biological relevance requires examination of the binding pose and its location relative to the known substrate-binding and catalytic region of α-amylase.

The CurPocket analysis revealed variation in the predicted volumes of the five binding cavities. Pocket C1 exhibited the largest volume (372 Å³), followed by C2 (307 Å³), C3 and C4 (175 Å³ each), and C5 (142 Å³). These values represent the estimated spatial dimensions of the identified cavities and provide an indication of their potential capacity to accommodate a ligand. All five pockets were evaluated using grid dimensions of 21 × 21 × 21 Å.

The interaction of Quercetin with α-amylase is relevant to its potential role in carbohydrate digestion and postprandial glucose regulation. α-Amylase catalyses the breakdown of starch into smaller carbohydrate products, which are subsequently converted into absorbable sugars. If Quercetin interacts with the substrate-binding region and inhibits enzyme activity, it may delay starch hydrolysis and reduce the rate of carbohydrate digestion. In the present study, the most favourable predicted docking energy was observed in pocket C5 (−7.5 kcal/mol). This result provides preliminary computational evidence that Quercetin may interact favourably with a predicted cavity of human pancreatic α-amylase.

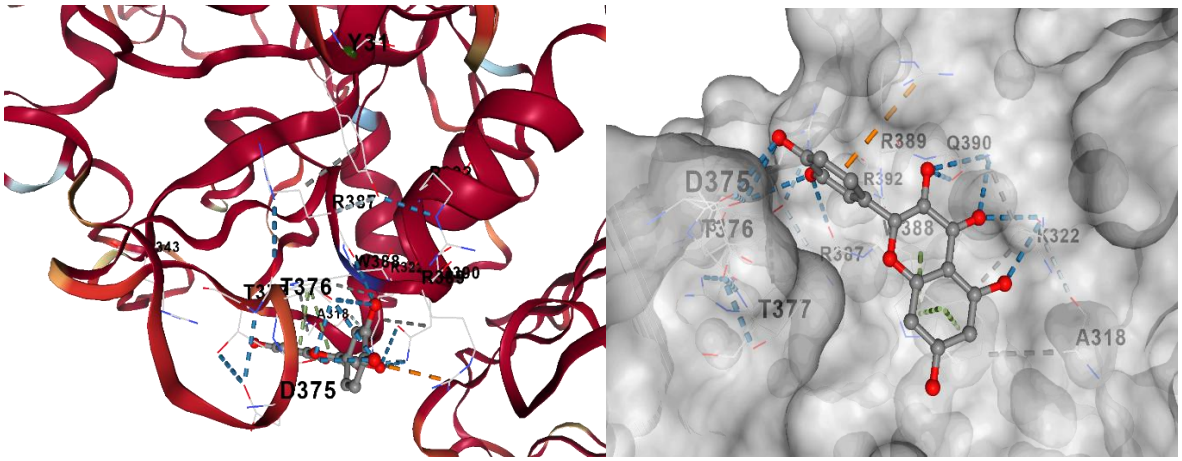

Figure 6. Representation Showing the Binding Orientation and Accommodation of Quercetin with α-Amylase (PDB ID: 5E0F)

4.7 Molecular Docking Analysis of Quercetin against α-Glucosidase (PDB ID: 3A4A)

α-Glucosidases are carbohydrate-hydrolysing enzymes involved in the terminal stages of carbohydrate digestion. They catalyse the hydrolysis of terminal α-linked glucose residues from oligosaccharides and disaccharides, releasing glucose for intestinal absorption. Inhibition of intestinal α-glucosidase can delay carbohydrate digestion and glucose absorption, thereby reducing postprandial blood glucose excursions.

The crystal structure PDB ID: 3A4A was selected for the present molecular docking investigation. An important structural detail is that 3A4A represents oligo-1,6-glucosidase (isomaltase) from Saccharomyces cerevisiae, rather than human intestinal α-glucosidase. It is an experimentally determined X-ray crystal structure with a resolution of 1.60 Å. The structure contains α-D-glucopyranose within the protein structure, providing a reference for examining the substrate-binding region. Five predicted pockets (C1–C5) were evaluated for Quercetin interaction. The corresponding

docking energies, pocket volumes, pocket-centre coordinates and grid dimensions are presented in Table 8.

Table 8. CurPocket analysis and molecular docking results of Quercetin against α-glucosidase (PDB ID: 3A4A)

CurPocket ID	Docking energy (kcal/mol)	Pocket volume (Å³)	Pocket centre (x, y, z)	Grid dimensions (Å)
C2	−8.5	573	(11, −11, 17)	21 × 21 × 21
C1	−7.7	737	(18, −28, 24)	21 × 21 × 21
C3	−7.6	285	(28, 17, −1)	21 × 21 × 21
C4	−6.9	94	(16, 0, −5)	21 × 21 × 21
C5	−6.4	83	(8, −30, 25)	21 × 21 × 21

The molecular docking analysis revealed predicted docking energies ranging from −6.4 to −8.5 kcal/mol across the five CurPocket-identified cavities. Among the evaluated pockets, C2 exhibited the most favourable docking energy of −8.5 kcal/mol, indicating the most favourable predicted interaction of Quercetin under the applied docking conditions. Pocket C1 demonstrated the next most favourable docking energy of −7.7 kcal/mol, followed by C3 with −7.6 kcal/mol. These results indicate that Quercetin produced favourable docking scores in more than one predicted binding cavity. Pocket C4 exhibited a docking energy of −6.9 kcal/mol, whereas C5 showed the least favourable value of −6.4 kcal/mol among the evaluated pockets. Interestingly, pocket C2 exhibited the most favourable docking energy despite having a smaller volume (573 Å³) than C1 (737 Å³). This observation indicates that pocket volume alone does not determine the predicted docking energy. Ligand orientation, steric complementarity, electrostatic contributions and the nature of interactions with surrounding amino acid residues can influence the docking result.

Pocket volume represents the estimated three-dimensional space available for ligand accommodation. Pocket C1 exhibited the largest volume of 737 Å³, followed by C2 with 573 Å³ and C3 with 285 Å³. The remaining cavities, C4 and C5, showed comparatively smaller volumes of 94 and 83 Å³, respectively. Although C1 represented the largest predicted cavity, C2 exhibited the most favourable docking energy. This finding suggests that the spatial dimensions of a binding cavity should not be considered independently when interpreting ligand-binding behaviour. The physicochemical compatibility between Quercetin and the amino acid residues lining the cavity, together with the ligand's orientation, may contribute to the predicted docking score. The smaller volumes of C4 and C5 describe more restricted predicted cavities. A uniform grid dimension of 21 × 21 × 21 Å was used for all five predicted binding pockets.

The favourable predicted docking energy observed for Quercetin in pocket C2 suggests a possible interaction with the selected α-glucosidase structure. If this interaction occurs within a functionally relevant substrate-binding region and is confirmed experimentally, Quercetin may potentially interfere with substrate recognition or catalytic activity. Such an effect could delay carbohydrate hydrolysis and contribute to the reduction of postprandial glucose excursions.

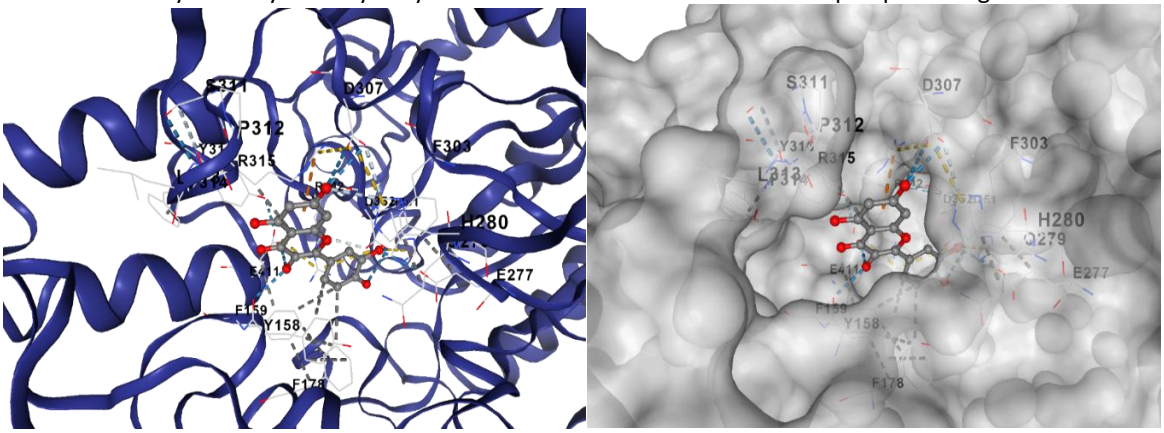

Figure 6. Representation Showing the Binding Orientation and Accommodation of Quercetin with α-Glucosidase (PDB ID: 3A4A)

5. Conclusion

The present study was undertaken to explore the potential antidiabetic relevance of two selected phytoconstituents, Abrine and Quercetin, through molecular docking analysis against multiple molecular targets associated with diabetes mellitus. The selected targets included α-amylase, α-glucosidase, dipeptidyl peptidase-4 (DPP-4), protein tyrosine

phosphatase 1B (PTP1B) and peroxisome proliferator-activated receptor gamma (PPAR-γ). The study involved the identification of potential binding cavities using CurPocket, followed by molecular docking to assess the predicted binding behaviour of the selected compounds. The results demonstrated that both compounds exhibited favourable predicted interactions with the investigated protein targets. Abrine showed its most favourable docking score against α-glucosidase (PDB ID: 3TOP), with a value of −7.4 kcal/mol in pocket C4. It also showed predicted interactions with DPP-4 (PDB ID: 5J3J), α-amylase (PDB ID: 4W93), PPAR-γ (PDB ID: 2PRG) and PTP1B (PDB ID: 2HNP), with the most favourable scores of −6.9, −6.6, −6.6 and −6.0 kcal/mol, respectively. Quercetin demonstrated its most favourable predicted interaction with α-glucosidase (PDB ID: 3A4A), exhibiting a docking score of −8.5 kcal/mol in pocket C2, followed by α-amylase (PDB ID: 5E0F), with a score of −7.5 kcal/mol in pocket C5. These findings provide preliminary computational evidence of the potential interactions of Abrine and Quercetin with molecular targets involved in carbohydrate digestion and glucose regulation. The predicted interactions with α-amylase and α-glucosidase suggest their possible relevance to the modulation of carbohydrate breakdown, whereas the docking results involving DPP-4, PTP1B and PPAR-γ provide additional molecular targets for investigating their potential role in glucose homeostasis and insulin signalling. The pocket analysis further indicated that favourable docking scores were not necessarily associated with the largest binding-pocket volumes, suggesting that the structural compatibility between the ligand and the binding cavity may influence the predicted docking behaviour. Overall, the molecular docking findings support the selection of Abrine and Quercetin for further investigation as potential antidiabetic phytoconstituents. However, these computational predictions should be interpreted cautiously, as docking analysis alone cannot confirm enzyme inhibition, receptor activation or in vivo antidiabetic efficacy. In particular, the α-glucosidase structure represented by PDB ID 3A4A corresponds to yeast isomaltase; therefore, further evaluation using an appropriate human intestinal α-glucosidase model is warranted. Future investigations should include in vitro enzyme inhibition assays, enzyme kinetic studies, molecular dynamics simulations and suitable in vivo pharmacological evaluations to establish the biological relevance and underlying mechanisms of the predicted interactions. Such experimental validation will be essential to determine the actual antidiabetic potential of these selected phytoconstituents and their possible contribution to the development of plant-derived therapeutic candidates.

References

1. Umamahesh B, Veeresham C. Antihyperglycemic and insulin secretagogue activities of Abrus precatorius leaf extract. Pharmacogn Res. 2016;8(4):303–308. doi:10.4103/0974-8490.188881.
2. Boye A, Barku VYA, Acheampong DO, Ofori EG. Abrus precatorius leaf extract reverses alloxan/nicotinamide-induced diabetes mellitus in rats through hormonal (insulin, GLP-1, and glucagon) and enzymatic (α-amylase/α-glucosidase) modulation. Biomed Res Int. 2021;2021:9920826. doi:10.1155/2021/9920826.
3. Boye A, et al. Glucose lowering and pancreato-protective effects of Abrus precatorius (L.) leaf extract in normoglycemic and STZ/nicotinamide-induced diabetic rats. J Ethnopharmacol. 2020;258:112918. doi:10.1016/j.jep.2020.112918.
4. Noor F, Rehman A, Ashfaq UA, Saleem MH, Okla MK, Al-Hashimi A, et al. Integrating network pharmacology and molecular docking approaches to decipher the multi-target pharmacological mechanism of Abrus precatorius L. acting on diabetes. Pharmaceuticals (Basel). 2022;15(4):414. doi:10.3390/ph15040414.
5. Lankatillake C, Huynh T, Dias DA. Abrus precatorius leaf extract stimulates insulin-mediated muscle glucose uptake: in vitro studies and phytochemical analysis. Planta Med. 2024;90(5):388–396. doi:10.1055/a-2281-0988.
6. Taofeek OO, Oyewole OM, Sulaimon LA, Sanusi SO, Akinnuoye PO, Dogara DV, et al. Abrus precatorius leaf bioactives: in vivo anti-diabetes mellitus type-1 activity, PPARA and SCD as novel targets. J Umm Al-Qura Univ Appl Sci. 2024;10:421–437. doi:10.1007/s43994-023-00113-x.
7. Jain A, Gupta PP. In silico comparative molecular docking study and analysis of glycyrrhizin from Abrus precatorius (L.) against antidiabetic activity. Eur J Med Plants. 2015;6(4):212–222. doi:10.9734/EJMP/2015/13855.
8. Zakłos-Szyda M, Majewska I, Redzynia M, Koziołkiewicz M. Antidiabetic effect of polyphenolic extracts from selected edible plants as α-amylase, α-glucosidase and PTP1B inhibitors, and β pancreatic cells cytoprotective agents—a comparative study. Curr Top Med Chem. 2015;15(23):2431–2444. doi:10.2174/1568026615666150619143051.
9. Huang X, Lin K, Liu S, Yang J, Zhao H, Zheng XH, et al. Combination of plant metabolites hinders starch digestion and glucose absorption while facilitating insulin sensitivity to diabetes. Front Pharmacol. 2024;15:1362150. doi:10.3389/fphar.2024.1362150.
10. In silico screening and identification of antidiabetic inhibitors sourced from phytochemicals of Philippine plants against four protein targets of diabetes (PTP1B, DPP-4, SGLT-2, and FBPase). Molecules. 2023;28(14):5301. doi:10.3390/molecules28145301.

11. Thamaraiselvi L, Selvankumar T, Wesely EG, Nathan VK. In silico molecular docking on bioactive compounds from Indian medicinal plants against type 2 diabetic target proteins: a computational approach. Indian J Pharm Sci. 2021;83(6):1273–1279. doi:10.36468/pharmaceutical-sciences.882.
12. Purnomo Y, Taufiq M, Wijaya AND, Hakim R. Molecular docking of soybean (Glycine max) seed and ginger (Zingiber officinale) rhizome components as anti-diabetic through inhibition of dipeptidyl peptidase 4 (DPP-4) and alpha-glucosidase enzymes. Trop J Nat Prod Res. 2021;5(10):1735–1742.
13. Okechukwu P, Sharma M, Tan WH, Chan HK, Chirara K, Gaurav A, et al. In-vitro anti-diabetic activity and in-silico studies of binding energies of palmatine with alpha-amylase, alpha-glucosidase and DPP-IV enzymes. Pharmacia. 2020;67(4):363–371. doi:10.3897/pharmacia.67.e58392.
14. Ghosh S, More P, Derle A, Patil AB, Markad P, Asok A, et al. Diosgenin from Dioscorea bulbifera: novel hit for treatment of type II diabetes mellitus with inhibitory activity against α-amylase and α-glucosidase. PLoS One. 2014;9(9):e106039. doi:10.1371/journal.pone.0106039.
15. Zhao Y, Kong KT, Jäger AK, Nielsen J, Staerk D. Quadruple high-resolution α-glucosidase/α-amylase/PTP1B/radical scavenging profiling combined with high-performance liquid chromatography–high-resolution mass spectrometry–solid-phase extraction–nuclear magnetic resonance spectroscopy for identification of antidiabetic constituents in crude root bark of Morus alba L. J Chromatogr A. 2018;1558:55–63. doi:10.1016/j.chroma.2018.04.041.
16. In vitro anti-diabetic activity of flavonoids and pheophytins from Allophylus cominia Sw. on PTP1B, DPPIV, α-glucosidase and α-amylase enzymes. J Ethnopharmacol. 2017;203:39–46. doi:10.1016/j.jep.2017.03.023.
17. Sun H, Wang D, Song X, Zhang Y, Ding W, Peng X, et al. Natural prenylchalconaringenins and prenylnaringenins as antidiabetic agents: α-glucosidase and α-amylase inhibition and in vivo antihyperglycemic and antihyperlipidemic effects. J Agric Food Chem. 2017;65(8):1574–1581. doi:10.1021/acs.jafc.6b05445.
18. Ortíz-Martinez DM, et al. Miconia sp. increases mRNA levels of PPAR gamma and inhibits alpha amylase and alpha glucosidase. Evid Based Complement Alternat Med. 2016;2016:5123519. doi:10.1155/2016/5123519.
19. Srinivasan K, Altemimi AB, Narayanaswamy R, Vasantha Srinivasan P, Najm MAA, Mahna N. GC-MS, alpha-amylase, and alpha-glucosidase inhibition and molecular docking analysis of selected phytoconstituents of small wild date palm fruit (Phoenix pusilla). Food Sci Nutr. 2023;11:5304–5317. doi:10.1002/fsn3.3489.
20. Okechukwu P, Sharma M, Tan WH, Chan HK, Chirara K, Gaurav A, et al. In-vitro anti-diabetic activity and in-silico studies of binding energies of palmatine with alpha-amylase, alpha-glucosidase and DPP-IV enzymes. Pharmacia. 2020;67(4):363–371. doi:10.3897/pharmacia.67.e58392.
21. Ojo OA, et al. Bioprospection of indigenous herbal formulations for diabetes care: in vitro, network pharmacology, and molecular dynamics studies. BMC Complement Med Ther. 2025;25(1):225. doi:10.1186/s12906-025-04980-1.
22. Wang J, Feng D, Xiang Y, Guo J, Huang N, Yu N, et al. Synthesis and inhibitory activity of euparin derivatives as potential dual inhibitors against α-glucosidase and protein tyrosine phosphatase 1B (PTP1B). Fitoterapia. 2023;169:105596. doi:10.1016/j.fitote.2023.105596.
23. Ali MY, Jannat S, Rahman MM. Investigation of C-glycosylated apigenin and luteolin derivatives' effects on protein tyrosine phosphatase 1B inhibition with molecular and cellular approaches. Comput Toxicol. 2021;17:100141. doi:10.1016/j.comtox.2020.100141.
24. Thiyagarajan G, Muthukumaran P, Sarath Kumar B, Muthusamy VS, Lakshmi BS. Selective inhibition of PTP1B by vitalboside A from Syzygium cumini enhances insulin sensitivity and attenuates lipid accumulation via partial agonism to PPARγ: in vitro and in silico investigation. Chem Biol Drug Des. 2016;88(2):302–312. doi:10.1111/cbdd.12757.
25. Okoh SO, et al. Identification of some bioactive compounds from Trigonella foenum-graecum as possible inhibitors of PPARγ for diabetes treatment through molecular docking studies, pharmacophore modelling and ADMET profiling: an in-silico study. PLoS One. 2023;18(5):e0284210. doi:10.1371/journal.pone.0284210.
26. Sajal H, et al. Computer-aided screening of phytoconstituents from Ocimum tenuiflorum against diabetes mellitus targeting DPP4 inhibition: a combination of molecular docking, molecular dynamics, and pharmacokinetics approaches. Molecules. 2022;27(16):5133. doi:10.3390/molecules27165133.
27. Characterization of plant-derived natural inhibitors of dipeptidyl peptidase-4 as potential antidiabetic agents: a computational study. Pharmaceuticals (Basel). 2024;16(4):483.
28. Identification of promising dipeptidyl peptidase-4 and protein tyrosine phosphatase 1B inhibitors from selected terpenoids through molecular modeling. Bioinformatics Advances. 2025;5(1):vbae205. doi:10.1093/bioadv/vbae205.
29. Repurposing dual-C-prenylated flavonoids as potent allosteric inhibitors of PTP1B: integrated phytochemical, enzymological, and in silico evidence. Int J Biol Macromol. 2025;316(Pt 1):144808. doi:10.1016/j.ijbiomac.2025.144808.
30. Identification of flavonoid C-glycosides as promising antidiabetics targeting protein tyrosine phosphatase 1B. Oxid Med Cell Longev. 2022;2022:6233217. doi:10.1155/2022/6233217.

31. Hsing HY, Rathnasamy S, Dianita R, Wahab HA. Docking-based virtual screening in search for natural PTP1B inhibitors in treating type-2 diabetes mellitus and obesity. Biomed Res Ther. 2020;7(1):3579–3592.
32. Khona P, Kabra U. Molecular docking and dynamic simulation analysis of natural polyphenols for identifying potential PTP1B inhibitors for type 2 diabetes. Indian J Chem. 2024;63(5):506–517. doi:10.56042/ijc.v63i5.9396.
33. Identification of some bioactive compounds from Trigonella foenum-graecum as possible inhibitors of PPARγ for diabetes treatment through molecular docking studies, pharmacophore modelling and ADMET profiling: an in-silico study. PLoS One. 2023;18(5):e0284210.
34. Mechanistic insights into antidiabetic potential of Ficus viren against multi organ specific diabetic targets: molecular docking, MDS, MM-GBSA analysis.
35. Characterization of plant-derived natural inhibitors of dipeptidyl peptidase-4 as potential antidiabetic agents: a computational study. Pharmaceuticals (Basel). 2024;16(4):483.
36. Haider AS, Ambatwar R, Khatik GL. Insights into PTP1B inhibitors as antidiabetic agents: current research and future perspectives. Eur J Med Chem. 2025;295:117791. doi:10.1016/j.ejmech.2025.117791.
37. Morris GM, Huey R, Lindstrom W, Sanner MF, Belew RK, Goodsell DS, et al. AutoDock4 and AutoDockTools4: automated docking with selective receptor flexibility. J Comput Chem. 2009;30(16):2785-2791. doi:10.1002/jcc.21256.
38. Paggi JM, Pandit A, Dror RO. The art and science of molecular docking. Annu Rev Biochem. 2024;93:389-410. doi:10.1146/annurev-biochem-030222-120000.
39. Nivatya HK, Singh A, Kumar N, Sonam, Sharma L, Singh V, et al. Assessing molecular docking tools: understanding drug discovery and design. Future J Pharm Sci. 2025;11:111. doi:10.1186/s43094-025-00862-y.
40. Grajales Ruiz DA, Negrisoli BF, Periquito ICC, Nascimento-Júnior NM, Gonçalves AM. SMILES2Docking: an open-source desktop workflow for ligand ionization, stereochemistry-aware preparation and semi-empirical 3D refinement. Mol Inform. 2026;45(9):e70053. doi:10.1002/minf.70053.
41. Cheminformatics identification of modulators of key carbohydrate-metabolizing enzymes from Crescentia cujete for type-2 diabetes mellitus intervention. J Diabetes Metab Disord. 2023. DOI: [10.1007/s40200-023-01249-7.
42. Investigation of α-glucosidase inhibition activity of Artabotrys sumatranus leaf extract using metabolomics, machine learning and molecular docking analysis. PLoS One. 2025;20(1):e0313592. DOI: [10.1371/journal.pone.0313592.
43. Computational study and in vitro α-glucosidase inhibitory effects of medicinal plants from a Thai folk remedy. Heliyon. 2021;7(9):e08078. DOI:[10.1016/j.heliyon.2021.e08078.
44. Identification of promising dipeptidyl peptidase-4 and protein tyrosine phosphatase 1B inhibitors from selected terpenoids through molecular modeling. Bioinformatics Advances. 2025. DOI: [10.1093/bioadv/vbae205.